

Inelastic neutron scattering, Raman, infrared and DFT theoretical studies on chloranilic acid[†]

A. Pawlukojć,¹ G. Bator,² L. Sobczyk,^{2*} E. Grech³ and J. Nowicka-Scheibe³

¹Joint Institute for Nuclear Research, 141 980 Dubna, Russia and Institute of Nuclear Chemistry and Technology, Dorodna 16, 03 195 Warsaw, Poland

²Faculty of Chemistry, University of Wrocław, Joliot-Curie 14, 50 383 Wrocław, Poland

³Institute of Chemistry and Environmental Protection, Technical University, Piastów Al. 12, 71 065 Szczecin, Poland

Received 12 November 2002; revised 26 February 2003; accepted 28 February 2003

ABSTRACT: The vibrational spectra of chloranilic acid (2,5-dihydroxy-3,6-dichloro-[1,4]-benzoquinone) in the solid state were studied by using inelastic neutron scattering (INS), infrared (IR) and Raman (R) spectroscopy. The spectra were compared with simulated spectra using the Gaussian and Climax programs. Sufficiently good agreement between the experimental and theoretical (DFT) spectra is observed although the calculations show that in the crystalline state a bifurcation of hydrogen bonds takes place. Relatively strong intermolecular interactions are noticeable when the experimental (x-ray) and calculated bond lengths and angles with participation of OH groups are compared. The studies of the deuterium isotope effect in the IR and R spectra enabled us to analyse the low-frequency out-of-plane vibrations and particularly the $\nu(\text{OH})$ and $\nu(\text{OD})$ modes. In the case of the $\nu(\text{OH})$ and $\nu(\text{OD})$ vibrations, one observes a strong asymmetry of the bands (low-frequency wings), which can be interpreted in terms of a coupling of the $\nu(\text{OH})$ mode with low-frequency ones damped by the lattice phonons and no fine structure of the $\nu(\text{OH})$ and $\nu(\text{OD})$ bands is observed. Copyright © 2003 John Wiley & Sons, Ltd.

KEYWORDS: chloranilic acid; vibrational spectra; DFT

INTRODUCTION

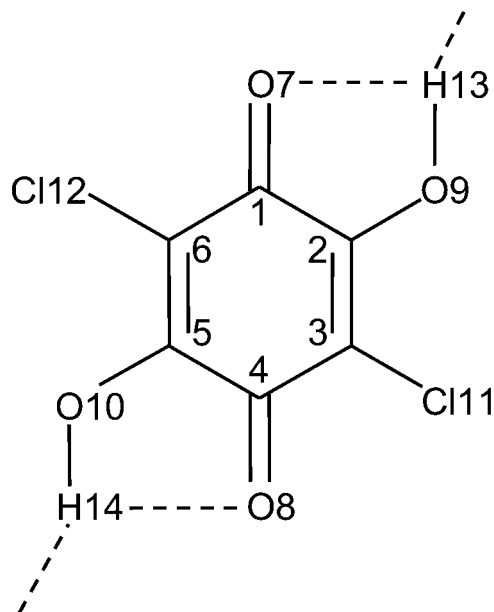
Benzoquinones, to which chloranilic acid belongs, are interesting systems from the point of view of electron-transfer reactions, which play an important role in biological systems.^{1–4} Chloranilic acid (2,5-dihydroxy-3,6-dichloro-[1,4]-benzoquinone, see Scheme 1) is interesting additionally as it can be a component of molecular complexes, being simultaneously an electron acceptor and proton donor [charge transfer (CT) and hydrogen bonded (HB) complexes]. There are already several reports related to the structure and properties of acid–base complexes with participation of chloranilic acid.^{5,6} Recently, attention has been paid to the possibility of its application in crystal engineering as a component of supramolecular synthons.^{7–9} The chemistry of complex compounds with participation of chloranilic acid (see, for example, Refs 10 and 11) also appeared rich. There have been reports on analytical and electrochemical applications of chloranilic acid^{12,13} and also spectroscopic studies of H-bonded complexes from the point of view of composition and proton-transfer process.^{14–16}

*Correspondence to: L. Sobczyk, Faculty of Chemistry, University of Wrocław, Joliot-Curie 14, 50 383 Wrocław, Poland.
E-mail: Sobczyk@wckwww.chem.uni.wroc.pl

[†]Dedicated to Professor M. Krygowski on the occasion of 65th birthday.
Contract/grant sponsor: Plenipotentiary Representative of the Polish Republic in JINR.

In the free molecule of chloranilic acid there are two five-membered H-bonded chelate rings. In the crystalline lattice, similarly to 2,5-dihydroxy-[1,4]-benzoquinone,¹⁷ there appear bifurcated hydrogen bonds, which lead to the creation of a layer structure¹⁸ consisting of infinite tapes with double O—H···O bridges. The interaction within the layers takes place through contacts between the chlorine and oxygen atoms. Bifurcated hydrogen bonds are the important structural element in solid chloranilic acid, similarly to 2,5-dihydroxy-[1,4]-benzoquinone: the OH groups are engaged in the formation of two hydrogen bridges. The interactions in the crystal do not change the symmetry of the molecules, i.e. it remains C_{2h} .

The influence of bifurcated hydrogen bonds on the dynamics of molecules was considered in previous papers devoted to 2,5-dihydroxy-[1,4]-benzoquinone.^{19,20} It has been shown that additional hydrogen bonds do not disturb substantially the dynamic pattern. For instance, the $\nu(\text{OH})$ frequency, which is sensitive to hydrogen bond interaction, is shifted from 3371 cm^{-1} in the gas phase to 3363 cm^{-1} and 3302 (3309) cm^{-1} in the solid state. For the phenol molecule in CHCl_3 solution this frequency is 3611 cm^{-1} .²¹ This means that the intramolecular hydrogen bond is relatively strong although somewhat weaker than the intermolecular bond. It should be mentioned that NMR studies of diotropic proton migration in 2,5-dihydroxy-[1,4]-benzoquinones showed relatively low



Scheme 1

barriers for proton transfer and can be interpreted in terms of a rather strong O—H \cdots O interaction.²²

In a previous paper,²⁰ the usefulness of the inelastic neutron scattering (INS) technique in studies of low-frequency vibrations ($<1000\text{ cm}^{-1}$) with participation of H atoms was demonstrated. The extension of these studies to the dichloro derivative was justified as the number of hydrogen atoms was reduced and thus the INS spectrum simplified. As is known, most contributions in INS spectra come from vibrations of hydrogen atoms. From inspection of the literature, the vibrational spectra of chloranilic acid, except for a few frequencies,^{14–16,23} have not been reported previously. Therefore, it seemed desirable to undertake detailed studies of INS and also infrared (IR) and Raman (R) spectra including analysis using density functional theory (DFT) calculations.

EXPERIMENTAL AND CALCULATIONS

Chloranilic acid (99%, Fluka) was crystallized from acetone. Deuteration was performed by twice recrystallization from CH_3OD . The degree of deuteration was ca 90%.

Neutron scattering data were collected at the pulsed reactor IBR-2 in Dubna using the inverted time-of-flight spectrometer NERA-PR.²⁴ Details relating to the installation are reported elsewhere.²⁵ A temperature of 22 K was maintained. The spectra were converted from neutrons per channel to phonon density of states $G(\omega)$ function per energy transfer by standard programs. At the energy transfers from 5 to 100 meV, the relative INS resolution was about 3%.

IR spectra were recorded at room temperature in Nujol or Fluorolube suspensions using either KBr or CsI plates

on a Bruker IFS 113v FT-IR spectrometer with a resolution of 2 cm^{-1} . Raman spectra of powder samples were recorded on a Nicolet Magna 860 FT Raman spectrometer. A diode-pumped Nd:YAG laser was excitation source, with a power of ca 200 mW. Backscattering geometry was applied. The resolution was set up for 2 cm^{-1} ; 512 scans were measured.

The structural parameters and frequencies, IR intensities and R activities of the molecule were calculated by using the Gaussian 98 program²⁶ at the HF, DFT B3LYP and DFT BLYP/6–31G(dp) levels. The PED% values at the BLYP/6–31G(dp) level were calculated using the GAMESS program.²⁷ The corresponding modes were defined by means of internal coordinates according to Pulay *et al.*²⁸ Mass-weighted normal vibrational coordinates were used to calculate the INS spectral profiles by the CLIMAX program,²⁹ adapted with author's permission to parameters of the NERA-PR spectrometer.

RESULTS AND DISCUSSION

A comparison of the calculated and experimental geometries of the chloranilic acid molecule is presented in Table 1. From these data, it clearly follows that considerable deformation in the solid state takes place but only with the fragment connected with the OH groups. The formation of intermolecular hydrogen bonds leads to a weakening of the intramolecular OHO bonds. This is particularly well manifested in the $\text{O7}\cdots\text{H13}$ distance and the O7—H13—O9 angle, which suggest a competitive attraction of the hydrogen atom towards a neighbouring molecule. Although in the crystalline lattice an elongation of $\text{O7}\cdots\text{O9}$ bridge to $2.673(5)\text{ \AA}$ takes place, we can still observe a relatively strong interaction comparable to that in the intermolecular bridge. As follows from the x-ray diffraction studies, the length of the intermolecular bridge is $2.769(4)\text{ \AA}$. The O9—H13 bond length determined by x-ray diffraction cannot be compared with the calculated value because, as is known,³⁰ the x-ray diffraction yields X—H bond lengths ca 0.1 \AA shorter than those determined by the neutron diffraction technique.

The vibrational frequencies measured by using three different techniques are compared with the calculated values in Table 2. Simultaneously, the assignments of the corresponding modes were performed based on the PED% values. Only in three cases was the assignment not successful, which is probably due to the overlapping of experimental bands. The appearance of either Raman or IR bands for a given mode corresponds to the C_{2h} symmetry of the molecules. On the other hand, almost all modes are reflected in the INS spectrum. The two lowest frequencies, which are overlapped by lattice phonons, are exceptions. Three other frequencies not observed in the INS spectrum have a very low intensity and overlap with neighbouring bands. Note that because of the limited

Table 1. Structural parameters of chloranilic acid (distances in Å, angles in degrees)

Coordinates	Calculated			Experiment: x-ray ¹⁸
	HF/6-31G**	B3LYP/6-31G**	BLYP/6-31G**	
C1—C2	1.516	1.523	1.528	1.501(7)
C2—C3	1.332	1.359	1.373	1.346(6)
C3—C4	1.464	1.451	1.464	1.445(6)
C1—O7	1.192	1.227	1.245	1.222(4)
C2—O9	1.310	1.321	1.340	1.322(5)
C3—Cl11	1.718	1.731	1.754	1.717(5)
O9—H13	0.952	0.986	1.003	0.90
O7...O9	2.589	2.570	2.588	2.673(4)
O7...H13	2.049	1.930	1.908	2.30
C6—C1—C2	118.6	118.8	118.5	117.9(3)
C1—C2—C3	121.8	122.5	122.7	120.9(4)
C2—C3—C4	119.5	118.7	118.7	121.2(5)
O7—C1—C2	116.5	115.4	115.4	118.2(4)
C1—C2—O9	114.3	113.2	113.0	116.6(4)
O9—C2—C3	123.9	124.3	124.3	122.7(4)
C2—C3—Cl11	122.5	122.4	122.6	120.9(4)
Cl11—C3—C4	117.9	118.8	118.7	117.9(3)
C3—C4—O8	124.9	125.8	126.0	123.8(4)
O7—H13—O9	114.2	120.1	122.4	104

resolution of the INS spectrometer, the bands above 1000 cm^{-1} cannot be interpreted.

Correlation between the calculated and experimental frequencies was accomplished for three different levels used in this study. For each method a constant scaling factor (SF) was assumed. The results of correlations are depicted in Fig. 1, which shows that both DFT methods yield reasonably good agreement between calculated and experimental data with high R^2 values.

A better comparison of the calculated and experimental spectra taking into account the band intensities can be made using Figs 2–4. The simulation of IR and R spectra was performed assuming the same band half-width of 8 cm^{-1} . The simulation of the INS spectra was performed by using the CLIMAX program.²⁹ The frequencies were calculated in all cases at the DFT B3LYP/6-31G** level assuming a scaling factor of 0.956.

Qualitative agreement between the calculated and experimental spectra can be seen, although it is clear that some bands are not very well reproduced. The largest differences are observed, however, in the intensities of bands. This relates particularly to the $1200\text{--}1400\text{ cm}^{-1}$ region. The bands in this region are assigned to complex modes with participation of $\delta(\text{OH})$ vibrations. In the experimental INS spectrum the $\gamma(\text{OH})$ band located around 700 cm^{-1} is distinguished, as expected. The $\gamma(\text{OH})$ peak in the simulated spectrum is not so sharp. One can only suppose that the accepted resolution of the spectrometer (3%) is somewhat underestimated in this region. Note that according to the expectation we should not resolve the transitions above 1000 cm^{-1} connected with $\delta(\text{OH})$ vibrations while the experiments allow us to draw some semi-quantitative conclusions for this spectral range.

Because the behaviour of bifurcated hydrogen bonds was one of the main aspects of our study, particular attention was paid to the $\nu(\text{OH})$ and $\gamma(\text{OH})$ vibrations and their isotope effect. The measured $\nu(\text{OH})$ value (the band maximum) in the IR region is 3243 cm^{-1} . The calculated value is somewhat higher, similar to that found for all other hydrogen-bonded systems. The difference depends markedly on the calculation method and the scaling factor used. One postulates that for frequencies of stretching vibrations with participation of hydrogen atoms the scaling factor should be smaller than that for lower frequency regions.³¹

The intermolecular $\text{OH}\cdots\text{O}$ hydrogen bond length for chloranilic acid is $2.769(4)\text{ \AA}$ compared with $2.728(4)\text{ \AA}$ for 2,5-dihydroxy-[1,4]-benzoquinone, although in the latter case the $\nu(\text{OH})$ value equals 3305 cm^{-1} , i.e. there is no correlation between bond lengths and $\nu(\text{OH})$ frequencies. As will be shown, the interaction strength expressed by the $\gamma(\text{OH})$ frequencies is consistent with expectation.

The $\nu(\text{OH})$ and $\nu(\text{OD})$ bands analysed for chloranilic acid are characterized by strong asymmetry with a wing in the low-frequency range, without any substructure, as shown in Fig. 5. Such a picture can be interpreted in terms of strong anharmonic coupling of a high-frequency vibration with low-frequency vibrations.^{32,33} However, a lack of substructure could indicate that the low-frequency vibrations are strongly damped, which can justify the application of the stochastic model of H-bond IR spectra.^{34,35} The application of such a model to medium-strong $\text{OH}\cdots\text{O}$ hydrogen-bonded systems leads to an asymmetric shape of the $\nu(\text{OH})$ band exactly the same as in this case.³⁶ The maximum of the $\nu(\text{OD})$ band is located at 2415 cm^{-1} , i.e. the isotopic ratio $\text{ISR} = 1.34$. This

Table 2. Calculated and experimental frequencies (cm^{-1}) for chloranilic acid

PED (%)	Symmetry	Calculated frequencies			Experimental frequencies ^a		
		HF/6-31G**	B3LYP/6-31G**	BLYP/6-31G**	INS	IR	R
Asym. torsion (99)	A_u	63	71 (0.05) ^b	72		77vw	
Asym. torsion (100)	A_u	88	103 (1.8)	108		115vw	
Puckering (100)	B_g	106	125 (0.03)	131	144	136vw	147vw
C-Cl bend. (83)	B_u	178	180 (0.2)	181	165		
C-Cl wagg. (62), C-O wagg. (30), C-Cl bend. (72), C-O bend. (13)	A_u	185	183 (1.88)	183	209		
Asym. def. (37), C-Cl str. (22), C-Cl bend. (11), C-O bend. (11)	A_g	199	201 (5.78)	203	219	215w	?
C-Cl wagg. (64), C-O wagg. (28)	A_g	263	269 (4.98)	271	246	222w	238w
C-O bend. (58), C-Cl str. (15), C-Cl str. (11)	B_g	288	298 (0.55)	303	290	336w	286w
C-O bend. (34), C-O bend. (27), C-C str. (16), C-Cl str. (10)	B_u	299	311 (22.5)	315	319		
C-O bend. (52), C-C str. (17), C-O bend. (13)	A_g	353	368 (8.0)	370	348		
Asym. def. (40), C=O bend. (18), C-C str. (17), C-O bend. (13)	B_u	367	384 (48.8)	387	385	384w	376w
C-O wagg. (60), C=O wagg. (21)	A_g	381	398 (1.6)	402	430		406m
C-C str. (31), C=C str. (18), asym. def. (17)	B_g	456	476 (0.69)	481	494		491sh
C-Cl str. (31), trigonal def. (30), C=O def. (15)	A_g	483	509 (24.9)	514			540m.
C-Cl wagg. (38), OH tors. (24)	B_u	512	535 (13.0)	537	542	?	
C=O wagg. (45), puckering (35)	A_u	568	555 (31.2)	556	583	572m	
C=O wagg. (55), asym. torsion (19)	B_g	677	682 (4.3)	682	669		?
C=O bend. (47), C-O bend. (32), C-Cl bend. (17)	A_u	688	691 (26.4)	701		753m?	
OH tors. (83)	A_g	717	719 (4.5)	759			787w
OH tors. (100)	A_u	534	726 (175.4)	781	731	693m	
C-Cl str. (35), trigonal def. (17), C=O bend. (15), C-O bend. (10)	B_g	544	751 (0.34)	782	771		769vw
C-Cl str. (52), C=C str. (39)	B_u	785	816 (105.5)	814		855m	
C-C str. (41), C-Cl bend. (13), C-O str. (12)	A_g	844	873 (6.8)	864	866		914vw
OH bend. (50), C-O str. (22)	B_u	913	949 (147.8)	949	934	984s	
C-O str. (19), OH bend. (18), C-C str. (14)	A_g	1171	1201 (58.9)	1204	1203		1241vw
C-C str. (48), C-O str. (29)	B_u	1150	1206 (97.9)	1211		1210w	
OH bend. (47), C-C str. (35)	A_g	1155	1236 (10.6)	1241	1234		1244w
C-O str. (40), C-C str. (26), OH bend. (19)	B_u	1220	1285 (269.7)	1279		1264s	
OH bend. (36), C-O str. (22), C-C str. (19)	B_u	1294	1342 (981.6)	1362	1354	1370s	1320w?
C=C str. (69)	A_g	1300	1370 (36.2)	1389		1376w	
C=C str. (63), C-O str. (10)	A_g	1588	1622 (224.5)	1605		1632s	1650s
C=O str. (89)	B_u	1602	1625 (177.2)	1618		1665s	
C=O str. (91)	B_u	1683	1666 (369.4)	1641			1672w
OH str. (100)	A_g	1691	1670 (60.0)	1655			3232vw
OH str. (100)	A_g	3471	3359 (171.3)	3260			
OH str. (100)	B_u	3474	3366 (315.5)	3270		3243s	

^a s, Strong; m, medium; w, weak; vw, very weak; sh, shoulder.^b Values in parentheses: either IR intensity in km mol^{-1} or Raman activity in $\text{\AA}^4/\text{AMU}$.

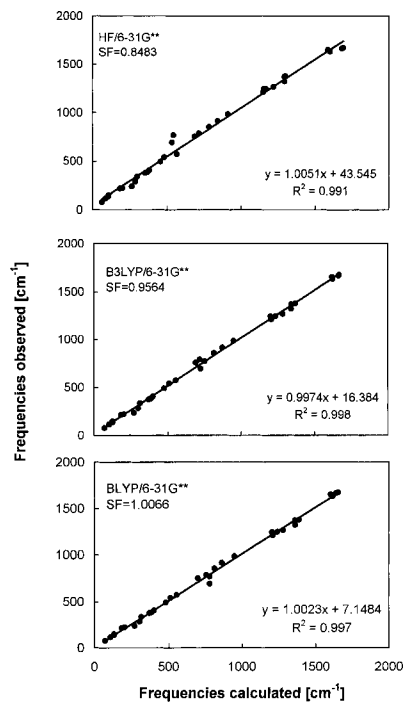


Figure 1. Correlation between calculated (for three different levels) and experimental frequencies

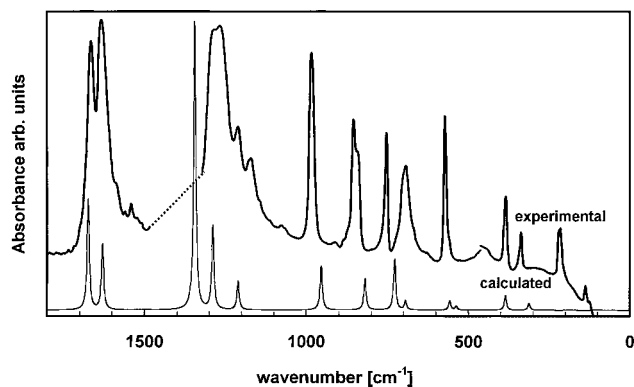


Figure 3. Calculated and experimental (upper) IR spectra of chloranilic acid (Nujol suspension)

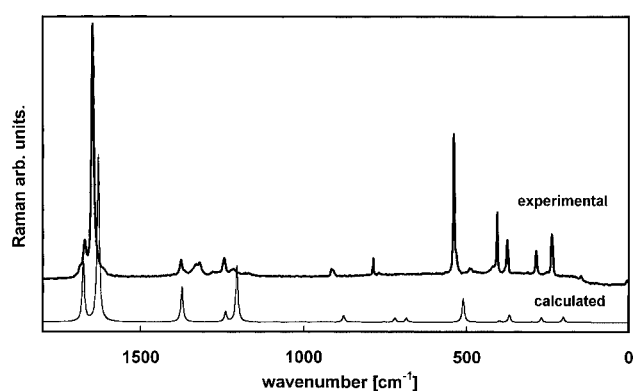


Figure 4. Calculated and experimental (upper) Raman spectra of powder chloranilic acid

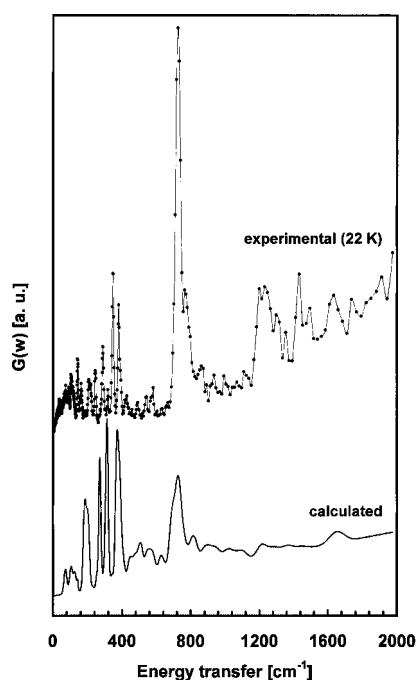


Figure 2. Calculated (upper) and experimental (22 K) INS spectra of powder chloranilic acid

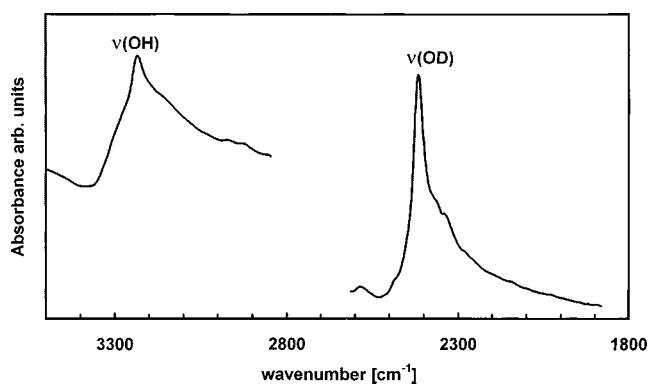


Figure 5. Shapes of $\nu(\text{OH})$ and $\nu(\text{OD})$ IR bands

implies a negligible deviation from the harmonic behaviour. For non-hydrogen-bonded phenol, $\text{ISR} = 1.35$.²¹

The D/H isotope effects in the fingerprint IR region are presented in Fig. 6. These effects are only slightly manifested in the region above 1200 cm^{-1} , where the $\delta(\text{OH})$ vibrations contribute, while they are spectacularly exposed in the region below 1100 cm^{-1} . The $\gamma(\text{OH})$ and

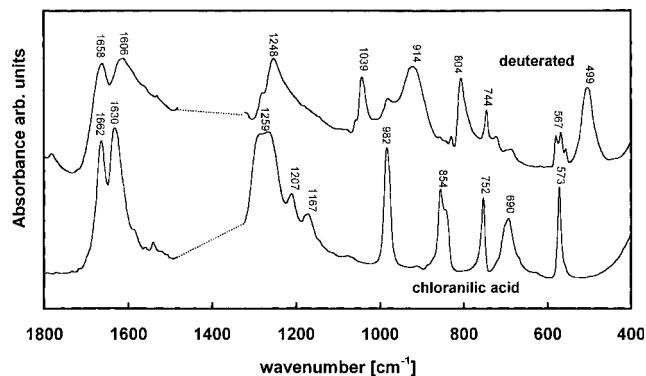


Figure 6. Comparison of IR spectra in the fingerprint region for non-deuterated and deuterated (upper) chloranilic acid (Nujol suspensions)

$\gamma(\text{OD})$ bands are localized at 693 and 504 cm^{-1} with $\text{ISR} = 1.37$. This means that these vibrations show almost pure harmonic behaviour. Other bands localized above 700 cm^{-1} undergo a substantial shift towards lower frequencies.

Very helpful for the interpretation of the isotope effect in the IR spectrum in the mid-frequency region were the calculations of frequencies and PED% for the deuterated compound. The calculations show that in the range below 500 cm^{-1} the isotope effect is negligibly small. The changes above 1600 cm^{-1} are typical of hydrogen-bonded systems. They arise from some contribution of $\delta(\text{OH})$ vibrations [and less from $\gamma(\text{OD})$ for the deuterated compound] with the main contribution of $\text{C}=\text{C}_{\text{str}}$ and $\text{C}=\text{O}_{\text{str}}$. In the spectrum of the deuterated compound very well-shaped intense bands appear at 1039 and 914 cm^{-1} , which are assigned to modes with a substantial contribution of $\delta(\text{OD})$ vibrations. Particularly characteristic is the band at 1039 cm^{-1} , to which the main contribution comes from $\delta(\text{OD})$ (40%). In the band at 914 cm^{-1} this contribution reaches 30%. There is a markedly lower contribution of $\delta(\text{OD})$ vibrations, according to calculation, for the band at 804 cm^{-1} (20%).

Acknowledgement

These studies were partly financed by the Plenipotentiary Representative of the Polish Republic in JINR.

REFERENCES

- Morton RA (ed). *Biochemistry of Quinones*. Academic Press: New York, 1965.
- Patai S (ed). *The Chemistry of the Quinoid Compounds*. Wiley: Chichester, 1974.

- Trumpower BL (ed). *Functions of Quinones in Energy Converting Systems*. Academic Press: New York, 1982.
- Kliuman JP, David M. *Annu. Rev. Biochem.* 1994; **63**: 299–330.
- Ishida H, Kashino S. *Acta Crystallogr., Sect. C* 1999; **55**: 1149–1152; 1999; **55**: 1714–1717; 2001; **57**: 476–479.
- Nihei TA, Ishimaru S, Ishida H, Ishihara H, Ikeda R. *Chem. Phys. Lett.* 2000; **329**: 7–14.
- Zaman MdB, Tomura M, Yamashita Y. *Chem. Commun.* 1999; 999–1000.
- Zaman MdB, Tomura M, Yamashita Y. *Org. Lett.* 2000; **2**: 273–275.
- Zaman MdB, Tomura M, Yamashita Y. *J. Org. Chem.* 2001; **66**: 5987–5995.
- Mostafa SI. *Transition Met. Chem.* 1999; **24**: 306–310.
- Abrahams BF, Lu KD, Moubaraki B, Murray KS, Robson R. *J. Chem. Soc., Dalton Trans.* 2000; 1793–1797.
- Zarebski J, Henze G. *Chem. Anal. (Warsaw)* 1998; **43**: 15–21.
- Osaka T, Momma T, Komoda S, Shiraiishi N, Kikuyama S, Yuasaa K. *Electrochemistry (Tokyo)* 1999; **67**: 238–242.
- Habeeb MM, Alwakil HA, El-Dissouky A, Fattah HA. *Pol. J. Chem.* 1995; **69**: 1428–1436.
- Habeeb M. *Spectrosc. Lett.* 1995; **28**: 573–579.
- Slifkin M, Smith B, Wolmsley R. *Spectrochim. Acta, Part A* 1969; **25**: 1479–1485.
- Semmlingsen D. *Acta Chem. Scand., Ser. B* 1977; **31**: 11–14.
- Andersen EK. *Acta Crystallogr.* 1967; **22**: 188–191.
- Szabó A, Kovacs A. *J. Mol. Struct.* 1999; **510**: 215–225.
- Pawlukojć A, Natkaniec I, Nowicka-Scheibe J, Grech E, Sobczyk L. *Spectrochim. Acta, Part A* 2003; **59**: 537–542.
- Rospenk M, Czarnik-Matusewicz B, Zeegers-Huyskens Th. *Spectrochim. Acta, Part A* 2001; **57**: 185–195.
- Bren VE, Chernoivanov VA, Konstantinovskii LE, Nivorozhkin LE, Zhdanov YuA, Minkin VI. *Dokl. Akad. Nauk SSSR*, 1980; **251**: 1129–1132.
- Issa YM. *Spectrochim. Acta, Part A* 1984; **40**: 137–140.
- Natkaniec I, Bragin SI, Brankowski I, Mayer J. In *Proceeding of the ICANS-XIII, Abington, 1993; RAL Report 94-025*, vol. I, 1993; 89.
- Pawlukojć A, Natkaniec I, Grech E, Baran J, Malarski Z, Sobczyk L. *Spectrochim. Acta, Part A* 1998; **54**: 439–448.
- Frisch MJ, Trucks GW, Schlegel HB, Scuseria GE, Robb MA, Cheeseman JR, Zakrzewski VG, Montgomery JA, Jr, Stratmann RE, Burant JC, Dapprich S, Millam JM, Daniels Ad, Kudin KN, Strain MC, Farkas O, Tomasi J, Barone V, Cossi M, Cammi R, Mennucci B, Pomelli C, Adamo C, Clifford S, Ochterski J, Petersson GA, Ayala PY, Cui Q, Morokuma K, Malick DK, Rabuck AD, Raghavachari K, Foresman JB, Cioslowski J, Ortiz JV, Baboul AG, Stefanov BB, Liu G, Liashenko A, Piskorz P, Komaromi I, Gomperts R, Martin RL, Fox DJ, Keith T, Al-Laham MA, Peng CY, Nanaayakkara A, Challacombe M, Gill PMW, Johnson B, Chen W, Wong MW, Anders JL, Gonzales C, Head-Gordon M, Replogle ES, Pople JA. *Gaussian 98, Revision A.5*. Gaussian: Pittsburgh, PA, 1998.
- Schmidt MW, Baldrige KK, Boatz JA, Elbert ST, Gordon MS, Jensen JH, Koseki S, Matsunaga N, Nguyen KA, Su SJ, Windus TL, Dupois M, Montgomery JA. *J. Comput. Chem.* 1993; **14**: 1347–1356.
- Pulay P, Forgasi G, Pang F, Boggs JE. *J. Am. Chem. Soc.* 1979; **101**: 2550–2560.
- Kearlay GJ. *Nucl. Instrum. Methods Phys. Res. A* 1995; **354**: 53–62.
- Olovsson I, Jönsson PG. In *The Hydrogen Bond*, vol. II, Schuster P, Zundel, G, Sandorfy CS (eds). North-Holland: Amsterdam, 1976; 393–456.
- Halls MD, Velkovski J, Schlegel HB. *Theor. Chem. Acc.* 2001; **105**: 413–442.
- Marechal Y, Witkowski A. *J. Chem. Phys.* 1968; **48**: 3697–3705.
- Wójcik MJ. *Int. J. Quantum Chem.* 1986; **29**: 855–866.
- Bratos S. *J. Chem. Phys.* 1975; **63**: 3499–3509.
- Robertson GN, Yarwood J. *Chem. Phys.* 1978; **32**: 267–282.
- Sobczyk L. *Mol. Phys. Rep.* 1996; **14**: 19–31.